

$K^+ \rightarrow \pi^+ \nu \bar{\nu}$ DECAY AND NP SEARCHES AT NA62*

SILVIA MARTELLOTTI

for the NA62 Collaboration[†]

INFN Laboratori Nazionali di Frascati
Via Enrico Fermi 40, Frascati (RM), Italy
silvia.martellotti@lnf.infn.it

(Received September 17, 2019)

The decay $K^+ \rightarrow \pi^+ \nu \bar{\nu}$ with a very precisely predicted branching ratio of less than 10^{-10} is one of the best candidates to reveal indirect effects of new physics at the highest mass scales. The NA62 experiment at CERN SPS is designed to measure the branching ratio of the $K^+ \rightarrow \pi^+ \nu \bar{\nu}$. In 2016, the first data set good for physics has been collected. The preliminary result on $\text{BR}(K^+ \rightarrow \pi^+ \nu \bar{\nu})$ from the full 2016 data set is presented here. Due to the high beam energy and hermetic detector coverage, NA62 has also the opportunity to directly search for a multitude of long-lived beyond-Standard-Model particles, such as dark photons, dark scalars, axion-like particles, and heavy neutral leptons. An overview of the broader NA62 physics program with status and prospects will be illustrated.

DOI:10.5506/APhysPolBSupp.13.95

1. The $K^+ \rightarrow \pi^+ \nu \bar{\nu}$ decay in the Standard Model

The $K^+ \rightarrow \pi^+ \nu \bar{\nu}$, ($K_{\pi\nu\bar{\nu}}$) decay is a flavour changing neutral current process proceeding through box and electroweak penguin diagrams. The process is very rare due to the quadratic GIM mechanism and strong Cabibbo suppression. The dominant contribution comes from the short-distance physics of the top quark loop, with a small charm quark contribution and long-distance corrections. This makes the $K_{\pi\nu\bar{\nu}}$ very clean theoretically and sensitive to physics beyond the Standard Model (SM), probing the highest mass scales among the rare meson decays [1]. The SM prediction using elements of the CKM matrix extracted from tree-level processes [2] is $\text{BR}(K^+ \rightarrow \pi^+ \nu \bar{\nu}) = (8.4 \pm 1.0) \times 10^{-11}$. The knowledge of the external

* Presented at “Excited QCD 2019”, Schladming, Austria, January 30–February 3, 2019.

[†] The list of NA62 Collaboration members can be found at the end of the article.

inputs dominate the uncertainties on the predictions. The present experimental measurement from the BNL E949 Collaboration [3], $\text{BR}(K^+ \rightarrow \pi\nu\bar{\nu}) = (17.3_{-10.5}^{+11.5}) \times 10^{-11}$, was obtained using stopped kaons. The big gap between theoretical precision and experimental error motivates a strong experimental effort to improve this measurement.

2. NA62 beam and detector

The fixed target NA62 experiment aims at measuring the branching ratio of the $K_{\pi\nu\bar{\nu}}$ decay with a 10% precision. A sample of about 10^{13} kaon decays should be collected in few years of data taking using the 400 GeV/c primary SPS proton beam. A maximum of 10% of background contamination is required, necessitating a background rejection factor of the order of 10^{12} . The beam impinges on a beryllium target producing secondary particles. A 100 m long beam line selects, collimates, focuses, and transports positive charged particles of (75.0 ± 0.8) GeV/c momentum to the evacuated fiducial decay volume of which the kaon component is 6%. The NA62 experimental apparatus is shown in Fig. 1. The KTAG is a differential Cherenkov detector filled with N_2 placed in the beam to identify and time-stamp kaons. It is followed by the Gigatracker (GTK) detector, composed of three silicon pixel stations of 6×3 cm² surface exposed to the full 750 MHz beam rate. The GTK is used to time-stamp and measure the momentum of the beam particles. The CHANTI detector tags hadronic beam–detector interactions in the last GTK station (GTK3). Downstream, the magnetic spectrometer made of four straw chambers and a dipole magnet between the second and third chamber is used to measure the momentum of the charged K^+ decay particles. A 17 m long RICH counter filled with neon gas is used to separate π^+ , μ^+ and e^+ . The time of charged particles is measured both with the RICH and with an array of scintillators (CHOD) located downstream of the RICH. Two hadronic calorimeters (MUV1 and MUV2) and a fast scintillator array (MUV3) provide further separation between π^+ and μ^+ . A set of

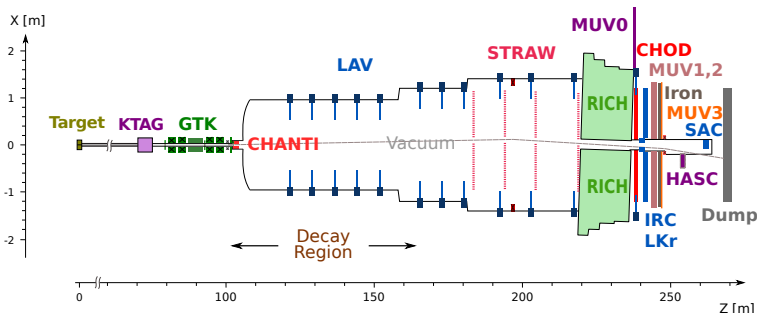


Fig. 1. Schematic layout of the NA62 experiment in the xz plane.

photons vetoes (LAVs, LKr, IRC, SAC) hermetically covers angles up to 50 mrad to reject extra electromagnetic activity. A detailed description of the apparatus and its performances can be found in [4].

3. The $K^+ \rightarrow \pi^+ \nu \bar{\nu}$ analysis

The analysis of the full 2016 data set is presented here, corresponding to $1.21(2) \times 10^{11}$ K^+ decays in the fiducial region. The $K_{\pi\nu\bar{\nu}}$ decay signature is one track in the initial and final state with two missing neutrinos. The main kinematic variable is $m_{\text{miss}}^2 \equiv (p_K - p_{\pi^+})^2$, p_K and p_{π^+} are the 4-momenta of the K^+ and π^+ , respectively. The analysis is performed in two separate regions: Region 1 (R1) between the $K^+ \rightarrow \mu^+ \nu_\mu (K_{\mu\nu})$ and $K^+ \rightarrow \pi^+ \pi^0 (K_{\pi\pi})$ contributions and Region 2 (R2) between $K_{\pi\pi}$ and $K^+ \rightarrow \pi^+ \pi^+ \pi^- (K_{\pi\pi\pi})$ contributions. The main backgrounds entering those regions are $K_{\mu\nu}$ and $K_{\pi\pi}$ decays through the non-Gaussian resolution and radiative tails; $K_{\pi\pi\pi}$ through the non-Gaussian resolution; $K^+ \rightarrow \pi^+ \pi^- e^+ \nu_e (K_{e4})$ and $K^+ \rightarrow l^+ \pi^0 \nu_l (K_{l3})$ decays ($l = \mu, e$); upstream background consisting of K^+ decays upstream of the GTK3 and inelastic beam–detector interactions. Each of the background processes requires different rejection procedure depending on kinematics and type of particles in the final state.

Events with the single track topology are selected using the downstream detectors STRAW, CHOD and RICH with a time coincidence resolution of 100 ps. The downstream track is then associated to an in-time kaon in the KTAG detector. The K^+ track is then reconstructed and time-stamped in the GTK detector. A kaon decay vertex is created at the intersection point of the GTK and STRAW tracks. The kaon decays within a 50 m fiducial region from 10 m downstream to GTK3 are selected. The π^+ tracks are identified by the calorimeters and the RICH counter providing 10^8 μ^+ suppression for 64% π^+ efficiency. The performances are measured on kinematically selected $K_{\pi\pi}$ and $K_{\mu\nu}$ decays on control-trigger data. Events passing the π^+ identification criteria are mainly $K_{\pi\pi}$ decays, which are further suppressed by rejecting in-time coincidences between the π^+ and energy deposits in the electromagnetic calorimeters LKr, LAVs, SAC, IRC. The resulting π^0 suppression is 3×10^{-8} , as measured from minimum bias and $K_{\pi\nu\bar{\nu}}$ -trigger streams before and after γ rejection, respectively.

Signal region definitions are driven by the m_{miss}^2 (STRAW, GTK) resolution $\sigma(m_{\text{miss}}^2) = 1 \times 10^{-3} \text{ GeV}^2/c^4$. To protect against kinematic misreconstruction, additional constraints are imposed on the m_{miss}^2 (RICH, GTK) computed by replacing the STRAW momentum with that measured by the RICH under a π^+ mass hypothesis and m_{miss}^2 (STRAW, Beam) computed by using nominal K^+ momentum. The total $K_{\pi\nu\bar{\nu}}$ acceptance in the signal regions after the complete selection is 4% (1% R1, 3% R2).

The probability of the $K_{\mu\nu}(K_{\pi\pi})$ decays to enter the signal regions defined by the three m_{miss}^2 is $3 \times 10^{-4}(1 \times 10^{-3})$. This kinematic suppression factor is used for the background estimation and is measured using $K_{\mu\nu}(K_{\pi\pi})$ decays on a control-trigger data sample. An MC simulation of 400 million generated $K^+ \rightarrow \pi^+\pi^-e^+\nu_e$ (K_{e4}) decays is used to estimate the expected background. The precision of the K_{e4} background estimation is limited by the size of the MC sample. The upstream background is estimated using a data driven method. The method is statistically limited, reflected in the large uncertainty dominating the overall background estimation. The background estimates in the signal regions are summarized in Table I, together with the signal events expectation obtained with MC.

TABLE I

Summary of the expected number of signal and background events in R1 and R2 after selection. Errors are added in quadrature to obtain the uncertainty on the total expected background.

Process	Expected events
$K^+ \rightarrow \pi^+\nu\bar{\nu}$ (SM)	$0.267 \pm 0.001_{\text{stat}} \pm 0.020_{\text{syst}} \pm 0.032_{\text{ext}}$
$K^+ \rightarrow \pi^+\pi^0(\gamma)$ IB	$0.064 \pm 0.007_{\text{stat}} \pm 0.006_{\text{syst}}$
$K^+ \rightarrow \mu^+\nu(\gamma)$ IB	$0.020 \pm 0.003_{\text{stat}} \pm 0.003_{\text{syst}}$
$K^+ \rightarrow \pi^+\pi^-e^+\nu$	$0.018^{+0.024}_{-0.017} _{\text{stat}} \pm 0.009_{\text{syst}}$
$K^+ \rightarrow \pi^+\pi^+\pi^-$	$0.002 \pm 0.001_{\text{stat}} \pm 0.002_{\text{syst}}$
Upstream background	$0.050^{+0.090}_{-0.030} _{\text{stat}}$
Total background	$0.15 \pm 0.09_{\text{stat}} \pm 0.01_{\text{syst}}$

The single event sensitivity for a SM $K_{\pi\nu\bar{\nu}}$ decay is $\text{SES} = (3.15 \pm 0.01_{\text{stat}} \pm 0.24_{\text{syst}}) \times 10^{-10}$, dominated by systematic uncertainty. The main uncertainty sources come from: random veto losses induced by the π^0 rejection procedure; stability of the SES estimation when varying the $\pi^+\pi^0$ normalization region; simulation of the π^+ losses due to interactions in the detector material upstream of the hodoscopes.

4. Results

One event is found in R2 after un-blinding the signal regions. The $K_{\pi\nu\bar{\nu}}$ candidate event (Fig. 2, left) has 15.3 GeV/ c momentum and is perfectly consistent with a π^+ track in the RICH detector (Fig. 2, right). Upper limit on the branching ratio of the $K^+ \rightarrow \pi^+\nu\bar{\nu}$ decay is obtained using the CL_s method [5]: $\text{BR}(K^+ \rightarrow \pi^+\nu\bar{\nu}) < 14 \times 10^{-10}$ at 95% C.L. The result, based on 2% of the total NA62 exposure in 2016–2018, demonstrates the validity of the

decay-in-flight technique in terms of background rejection and in view of the measurement in progress, with both hardware and analysis improvements, using the full data sample.

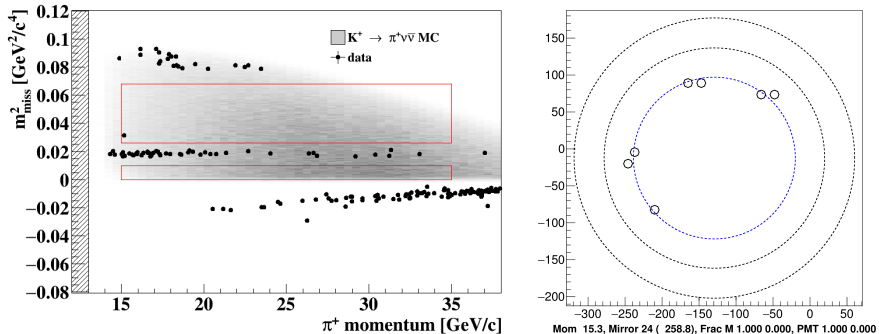


Fig. 2. (Colour on-line) Left: m^2_{miss} as a function of P_{π^+} (dots) after the complete $K^+ \rightarrow \pi^+ \nu \bar{\nu}$ selection is applied, but the cuts on m^2_{miss} and P_{π^+} . Grey area corresponds to the distribution of $K^+ \rightarrow \pi^+ \nu \bar{\nu}$ MC events. Black/red lines define signal regions. One event is observed in R2. Right: Position of the hits in the RICH event display associated to the π^+ track for the observed event in R2. Circles illustrate e^+ , μ^+ and π^+ hypothesis, showing a perfect agreement with a π^+ (innermost ring).

5. Exotic searches

Redundant particle identification systems and hermetic, highly-efficient photon veto detectors, together with the high-intensity beam and flexible trigger system, make NA62 particularly suitable for searching for the decays of exotic, long-lived particles [6] produced in the target and dump collimator or in the decays of kaons in the beam. Analysis of data for all the searches mentioned in the following is in progress.

NA62 can search for dark photons [7] with no decays to SM particles. Figure 3, left, shows preliminary 90% C.L. exclusion limits in the mass-coupling ($m_{A'}$, ϵ) plane for invisible dark photons searched in $K^+ \rightarrow \pi^+ \pi^0$ with $\pi^0 \rightarrow \gamma A'$, in which the missing-mass distribution for candidate events with one track, one photon, and missing energy is examined for evidence of the peak from the A' . This result was obtained with a sample of $1.5 \times 10^{10} K^+$ decays, the 5% of the 2016 data sample. NA62 can also search for dark photons produced in the target that decay to $e^+ e^-$ or $\mu^+ \mu^-$ inside the fiducial volume. Figure 3, right, shows the sensitivity estimate obtained for 10^{18} protons on target (p.o.t.) with both these channels. Zero background is assumed. This assumption has been proven to be valid up to exposures of 10^{15} protons with data collected with parasitic ee and $\mu\mu$ triggers.

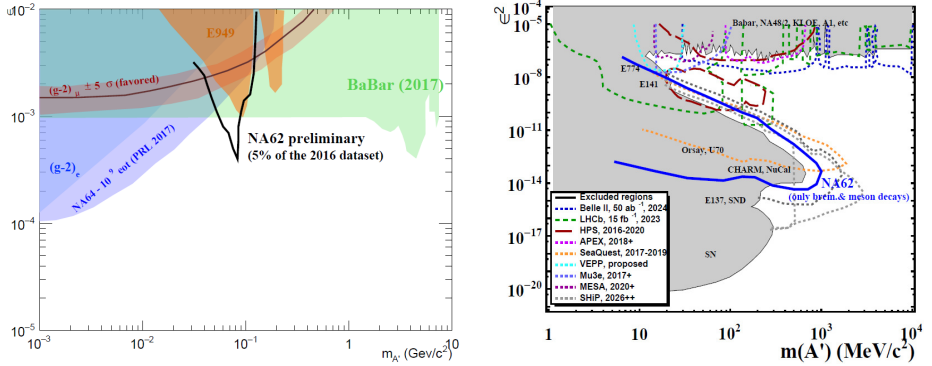


Fig. 3. Left: Preliminary 90% C.L. exclusion limits in the $(m_{A'}, \epsilon)$ plane for dark photons A' with no decays to SM particles, from a 5% subset of NA62 2016 data. Right: Estimated NA62 90% C.L. exclusion limits in $(m_{A'}, \epsilon)$ assuming 10^{18} p.o.t. and zero background for dark photons A' decaying to e^+e^- or $\mu^+\mu^-$.

Searches of axion-like particles (ALPs) [8] produced by the Primakoff process ($\gamma\gamma$ fusion) in interactions in the dump may also be performed in NA62. In a dedicated running, the target may be lifted and the copper collimators closed, so that the whole beam interacts in a higher Z material closer to the detector, increasing the sensitivity. Samples of $O(10^{15})$ p.o.t. have been collected in dump mode for sensitivity studies. Figure 4, left, shows an estimate of the 90% C.L. exclusion that NA62 could obtain with 10^{18} p.o.t. and zero background. NA62 can search for Heavy Neutral Leptons (Ns) [9] produced in kaon decays in the M_{miss} spectrum for $K^+ \rightarrow l^+ N$, as discussed in detail in [10]. In addition, NA62 can search for Ns produced in the dump

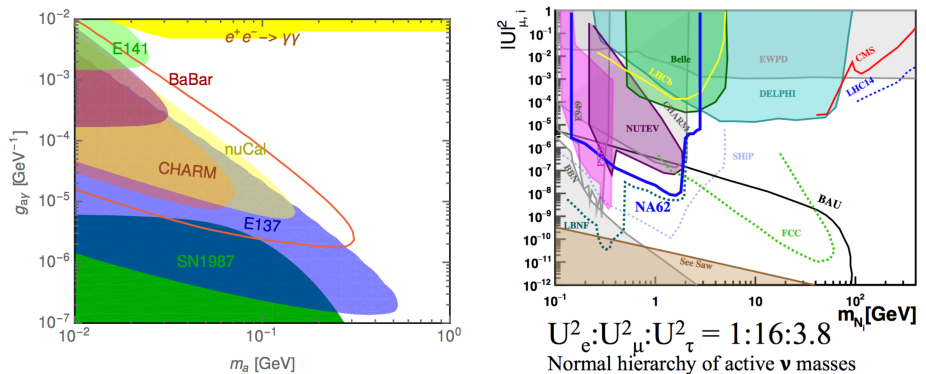


Fig. 4. Left: NA62 estimated 90% C.L. exclusion limits in the $(m_a, g_{a\gamma})$ plane, assuming 10^{18} p.o.t. and zero background, for axion-like particles decaying to $\gamma\gamma$. Right: NA62 estimated 90% C.L. exclusion limits in the $(m_N, |U_a^2|)$ plane, in the scenario in which the couplings to SM neutrino- μ is dominant.

that decay to two charged particles. Figure 4 shows NA62 estimated 90% C.L. exclusion for 10^{18} p.o.t. in the plane of $|U_\alpha|$ vs. m_N , where U_α is the element of the neutrino-mixing matrix relating N to SM neutrino $\alpha \in e, \mu, \tau$. The sensitivity is shown for one of the coupling scenarios discussed in [11]. In 2017, NA62 took 10^{17} p.o.t. with a $\pi\mu$ parasitic trigger and a few 10^{16} p.o.t. with a πe parasitic trigger.

REFERENCES

- [1] M. Blanke *et al.*, *J. High Energy Phys.* **0903**, 108 (2009); A.J. Buras, D. Buttazzo, R. Knegjens, *J. High Energy Phys.* **1511**, 166 (2015); T. Blažek, P. Maták, *Int. J. Mod. Phys.* **29**, 1450162 (2014); G. Isidori *et al.*, *J. High Energy Phys.* **0608**, 064 (2006); M. Blanke, A.J. Buras, S. Recksiegel, *Eur. Phys. J. C* **76**, 182 (2016); M. Bordone, D. Buttazzo, G. Isidori, J. Monnard, *Eur. Phys. J. C* **77**, 618 (2017).
- [2] A.J. Buras, D. Buttazzo, J. Girrbach-Noe, R. Knegjens, *J. High Energy Phys.* **1511**, 033 (2015).
- [3] E949 Collaboration, *Phys. Rev. D* **79**, 092004 (2009).
- [4] NA62 Collaboration, *JINST* **12**, P05025 (2017).
- [5] A.L. Read, *J. Phys. G: Nucl. Part. Phys.* **28**, 2693 (2002).
- [6] M. Pospelov, A. Ritz, M. Voloshin, *Phys. Rev. D* **78**, 115012 (2008).
- [7] M. Pospelov, *Phys. Rev. D* **80**, 095002 (2009).
- [8] Y. Nomura, J. Thaler, *Phys. Rev. D* **79**, 075008 (2009).
- [9] T. Asaka, M. Shaposhnikov, *Phys. Lett. B* **620**, 17 (2005).
- [10] NA62 Collaboration, *Phys. Lett. B* **778**, 137 (2018).
- [11] D. Gorbunov, M. Shaposhnikov, *J. High Energy Phys.* **0710**, 015 (2007).

The list of NA62 Collaboration members: R. Aliberti, F. Ambrosino, R. Ammendola, B. Angelucci, A. Antonelli, G. Anzivino, R. Arcidiacono, T. Bache, M. Barbanera, J. Bernhard, A. Biagioni, L. Bician, C. Biino, A. Bizzeti, T. Blazek, B. Bloch-Devaux, V. Bonaiuto, M. Boretto, M. Bragadireanu, D. Britton, F. Brizioli, M.B. Brunetti, D. Bryman, F. Bucci, T. Capussela, J. Carmignani, A. Ceccucci, P. Cenci, V. Cerny, C. Cerri, B. Checucci, A. Conovaloff, P. Cooper, E. Cortina Gil, M. Corvino, F. Costantini, A. Cotta Ramusino, D. Coward, G. D'Agostini, J. Dainton, P. Dalpiaz, H. Danielsson, N. De Simone, D. Di Filippo, L. Di Lella, N. Doble, B. Dobrich, F. Duval, V. Duk, J. Engelfried, T. Enik, N. Estrada-Tristan, V. Falaleev, R. Fantechi, V. Fascianelli, L. Federici, S. Fedotov, A. Filippi, M. Fiorini, J. Fry, J. Fu, A. Fucci, L. Fulton, E. Gamberini, L. Gatignon, G. Georgiev, S. Ghinescu, A. Gianoli, M. Giorgi, S. Giudici, F. Gonnella, E. Goudzovski, C. Graham, R. Guida, E. Gushchin, F. Hahn, H. Heath, E.B. Holzer, T. Husek, O. Hutanu,

D. Hutchcroft, L. Iacobuzio, E. Iacopini, E. Imbergamo, B. Jenninger, J. Jerhot, R.W. Jones, K. Kampf, V. Kekelidze, S. Kholodenko, G. Khoraiuli, A. Khotyantsev, A. Kleimenova, A. Korotkova, M. Koval, V. Kozhuharov, Z. Kucerova, Y. Kudenko, J. Kunze, V. Kurochka, V. Kurshetsov, G. Lanfranchi, G. Lamanna, E. Lari, G. Latino, P. Laycock, C. Lazzeroni, M. Lenti, G. Lehmann Miotto, E. Leonardi, P. Lichard, L. Litov, R. Lollini, D. Lomidze, A. Lonardo, P. Lubrano, M. Lupi, N. Lurkin, D. Madigozhin, I. Mannelli, G. Mannocchi, A. Mapelli, F. Marchetto, R. Marchevski, S. Martellotti, P. Massarotti, K. Massri, E. Maurice, M. Medvedeva, A. Mefodev, E. Menichetti, E. Migliore, E. Minucci, M. Mirra, M. Misheva, N. Molokanova, M. Moulson, S. Movchan, M. Napolitano, I. Neri, F. Newson, A. Norton, M. Noy, T. Numao, V. Obraztsov, A. Ostankov, S. Padolski, R. Page, V. Palladino, A. Parenti, C. Parkinson, E. Pedreschi, M. Pepe, M. Perrin-Terrin, L. Peruzzo, P. Petrov, Y. Petrov, F. Petrucci, R. Piandani, M. Piccini, J. Pinzino, I. Polenkevich, L. Pontisso, Yu. Potrebenikov, D. Protopopescu, M. Raggi, A. Romano, P. Rubin, G. Ruggiero, V. Ryjov, A. Salamon, C. Santoni, G. Saracino, F. Sargeni, S. Schuchmann, V. Semenov, A. Sergi, A. Shaikhiev, S. Shkarovskiy, D. Soldi, V. Sugonyaev, M. Sozzi, T. Spadaro, F. Spinella, A. Sturgess, J. Swallow, S. Trilov, P. Valente, B. Velghe, S. Venditti, P. Vicini, R. Volpe, M. Vormstein, H. Wahl, R. Wanke, B. Wrona, O. Yushchenko, M. Zamkovsky, A. Zinchenko.